

Alternate Layers of Cobalt Doped Tungsten Oxide and Reduced Graphene Oxide Composite as Electrode Material for Supercapacitor

P. DHILIP, M. NITHTHIYANANDAM, N. SETHUPATHI and P. MAHALINGAM*

Department of Chemistry, Arignar Anna Government Arts College, Namakkal-637002, India

*Corresponding author: E-mail: ponmahanano@gmail.com

Received: 27 September 2019;

Accepted: 20 November 2019;

Published online: 25 February 2020;

AJC-19798

Composites consist of layers of cobalt doped tungsten oxide and reduced graphitic oxide was prepared using jet nebulized spray pyrolysis technique. A mixture of ammonium tungstate and cobalt acetate solution was coated on glass substrate at 380 °C using jet nebulized spray pyrolysis technique. Spray technique is used to form the reduced graphene oxide (rGO) layer over the first layer and again ammonium tungstate and cobalt acetate solution coated over the surface of rGO and then calcined in nitrogen atmosphere at 450 °C for 2 h. The composite were characterized using XRD, SEM, PL, CV and EIS studies. The SEM and XRD reveal the layered structure. Cyclic voltammetry reveals the high specific capacitance 500 Fg⁻¹ at 5 mV s⁻¹ scan rate for 2 M Na₂SO₄ as electrolyte. Layered structure of CoWO₄/rGO/CoWO₄ composite enhances the specific capacitance. EIS gives the electrical series resistance of 7.9 Ω. The layered CoWO₄/rGO/CoWO₄ composite can be suitable electrode materials for supercapacitor.

Keywords: Layered composite, Doped metal oxide, rGO, Spray technique, Supercapacitor.

INTRODUCTION

Supercapacitor is one of the emerging energy storage devices in recent years. Long cycle life, charge/discharge process, high energy and power densities are the favours of supercapacitor [1]. The supercapacitor devices are classified into three types depending upon design of electrode namely electrochemical double layer capacitor (EDLC), pseudo-capacitor and hybrid capacitor [2]. Electrochemical properties of the supercapacitor mainly depend on used electrode material [3]. Numbers of materials were used as electrode for supercapacitor. Electrochemical double layer capacitor electrodes consist of carbon based materials and pseudo capacitor electrodes consist of metal oxide and conducting polymers [4]. Transition metal oxide is good electrode material for pseudo capacitor because transition metal oxides have a high pseudo capacitive type, various oxidation states, high power and mass density [5]. Electrochemical properties of the single metal oxide material were improved to introduce doping of another metal oxide or metal elements into the single metal oxide [6]. Mixed metal oxide material is good electrode material for lithium ion batteries and electrical capacitors.

Mixed metal oxides have high electrical activity sites and their synergistic effect influence to improve the high specific capacitance [7]. Mixed transition metal oxide pseudo capacitor shows a good performance compare with single metal oxide electrode system, due to different oxidation state, various Faradic redox reactions. Mixed metal oxides of NiMoO₄, NiCoO₄ and CoMoO₄ material shows a higher electrical conductivity than single transition metal oxide materials [8]. At the same time mixed metal oxide materials performance still suffer from poor electrical conductivity, poor cycling stability and so the researchers move towards hybrid capacitor [9]. Hybrid capacitor consists of carbon based material and metal oxide or polymer based materials in the same system. This synergistic effect improves the performance of the capacitor and combine properties of EDLC and pseudo capacitor [10]. Hybrid capacitor carbon based materials provide a faradic charge storage mechanism and metal oxide or conducting polymer materials exhibit non faradic charge storage mechanism of pseudo capacitive behaviour, this both type of storage mechanism provide a high specific capacitance and power density without losing their energy density of materials [11]. Number of metal oxide and carbon based materials were used

to construct electrode for supercapacitor like RuO₂, NiO, MnO₂, CNT, graphene and activated carbons [12]. Tungsten oxide and cobalt oxide are the most known electrode material for supercapacitor. Tungsten oxide have the outstanding properties of high photo activity, no-photo corrosion and good electron transport. Co₃O₄ shows the large surface area, high conductivity and good reversibility properties [13,14]. Recently cobalt doped tungsten oxide material have great attention in the field of sensors, catalysts and supercapacitors because this material provide a number of applications in the room temperature [15]. Hydrothermal method, spray pyrolysis and various techniques were used to prepare cobalt doped tungsten oxide material with controllable size and shape [16]. One of the promising carbon based electrode material is reduced graphene oxide (rGO) for its high mechanical stability, electrical conductivity, large surface area. These unique properties of graphene oxide lead to use in catalysts, fuel cell, gas sensors and supercapacitors [17]. Transition metal oxide electrochemical properties were remarkably improved combining of graphene into metal oxide material. Transition metal oxide and graphene composite have good cyclic stability and rate capability due to enhanced electrical conductivity and contact area between the electrode/electrolyte [18]. Graphene films were constructed using various techniques but film affected in architecture and their properties. This draw back leads to the loss of active sites in surface area of the graphene. The composite material as layer by layer architecture were prepared using jet nebulized spray pyrolysis technique. This method is useful for easy doping of required composition and also grows nano level thin film with uniform and required thickness. Layer by layer method not only influence the thickness of the film, structure and flexibility it also initiate to reach the good chemical stability and charge/discharge process [19,20]. Recently manganese oxide and reduced graphene oxide were synthesized by silar method. This composite used as electrode for supercapacitor and produce a high specific capacitance, high power and energy density [21]. Electrolyte is one of the most important factors to define the working voltage of prepared supercapacitor and three types of electrolytes are presented namely organic, ionic and aqueous electrolytes. Organic and ionic electrolytes have poor conductivity and high viscosity. But aqueous electrolytes have poor viscosity and high conductivity than others, many pseudo capacitors device worked with aqueous electrolyte and achieve an enhanced electrochemical performance [22]. In this article, alternate layers of cobalt doped tungsten oxide and reduced graphene oxide layers preparation using jet nebulized spray pyrolysis technique and characterization of the material for supercapacitor electrode are discussed.

EXPERIMENTAL

Cobalt acetate [Co(CH₃COO)₂·4H₂O] and ammonium tungstate [(NH₄)₂WO₃]·2H₂O were used to prepare cobalt doped tungsten oxide layer by jet nebulized spray pyrolysis technique. In this technique precursor solution is converted into aerosol mist by double collision process. Jet nebulizer technique consists of jet nebulizer assembly, air compressor with pressure controller, electrical heater and mist container tube. Jet nebulizer is one of the atomization mechanism and

that convert the solution to micron size droplets and aerosol mist with help of compressed air. This mists and micron droplets are passed through the guide tube to heater and deposit over the substrate surface and form the metal oxide thin films on surface of the substrate [20]. Graphene oxide was prepared from graphite flakes by Hummers method. Ammonium tungstate (0.2 mmol) and cobalt acetate (0.2 mmol) solutions mixed in 2:1 ratio was ultra sonicated for 30 min. 6 mL of the mixture is coated over the glass substrate at optimized temperature of 380 °C. Prepared graphene oxide suspended in ethanol was coated over the thin film layer of ammonium tungstate cobalt acetate composite by fabricated sprayer with a nozzle size of 1mm diameter. Third layer of ammonium tungstate cobalt acetate composite coated over the surface of graphene oxide layer. The prepared composite was calcinated in nitrogen atmosphere at 450 °C for 2 h. During calcination, ammonium tungstate, cobalt acetate and layer of the graphene oxide undergo reduction to form CoWO₄/rGO/CoWO₄. The same procedure was used to prepare undoped layer structure of WO₃/rGO/WO₃. The layered composite materials are characterized using XRD, PL, SEM, CV and EIS techniques.

RESULTS AND DISCUSSION

XRD pattern of prepared materials of reduced graphene oxide (rGO), layers of WO₃/rGO/WO₃ and CoWO₄/rGO/CoWO₄ composites are presented in Fig. 1. Reduced graphene oxide (rGO) XRD pattern (Fig. 1a) reveals the peak at 26.42° with d-spacing 3.3735 Å. The characteristics peak of graphene oxide at 11.08° disappeared and appearance a peak at 26.42° confirms the graphene oxides are reduced to rGO under the experimental conditions [23]. Layered materials of undoped tungsten oxide and reduced graphitic oxides XRD pattern (Fig. 1b) well agreed with standard JCPDS No. 89-8764 and exhibits a tetragonal phase with polycrystalline structure.

Cobalt doped tungsten oxide and reduced graphene oxide composite XRD pattern (Fig. 1c) shows a characteristic peak at 2θ value of 10.63°, 26.48°, 29.50°, 35.51°, 36.46°, 38.59°, 42.36° and 61.41°. The peak at 26.48° corresponds to the reduced graphene oxides in composite. The pattern is closely matched with standard JCPDS No. 15-0867 with monoclinic phase of CoWO₄. Doped material peaks are slightly shifted in their position compare with undoped material, this result indicates the cobalt ions are into the tungsten oxide lattice due to the smaller atomic radius of cobalt ion (1.16 pm) compared with tungsten atomic radius (1.5 pm) [24]. Layers CoWO₄/rGO/CoWO₄ composites broad peak of rGO indicates reduced graphene oxides are presented in disorderly stacked structure [25]. The average particle size of cobalt doped tungsten oxide calculated using Debye Scherrer equation was found to be 60 nm.

Optical properties of the prepared composites were characterized using photoluminescence spectroscopy (PL). Fig. 2 shows the PL spectra of layered composite of undoped WO₃/rGO/WO₃ (Fig. 2a) and doped CoWO₄/rGO/CoWO₄ composite (Fig. 2b). Undoped and doped composite shows a peaks at 377.07, 405, 448.92, 471.95, 488.04, 496.05, 505.97, 521.03 and 361.07, 376, 405, 438.92, 451.05, 468.95, 493.92, 505.97, 521.94 nm, respectively. Doped material shows a UV

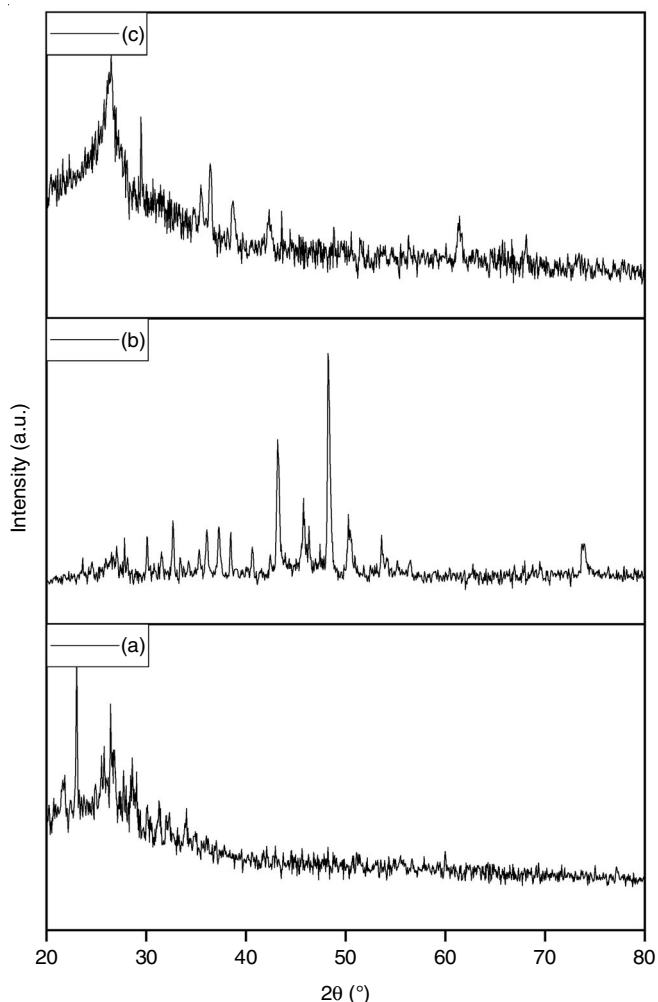


Fig. 1. XRD pattern of (a) rGO, (b) $\text{WO}_3/\text{rGO}/\text{WO}_3$ and (c) $\text{CoWO}_4/\text{rGO}/\text{CoWO}_4$ composites

emission peak at 361.07 nm due to the presence of band to band transition. The blue emission appear at 405 and 438.92 nm for doped composite is related to existence of doped metal ion Co^{2+} in the crystalline lattice and it facilitate the transition between blocked conduction band to unblocked valence band. The doped composite exhibits a green emission peak at 521 nm. The appearance of green emission may be due to different luminescence centers and oxygen vacancies in doped composites [13,24]. Band gap energy of the prepared doped and undoped composite is 2.38 and 2.48 eV, doped material band gap energy value is lees then that of undoped material because metal doping provides a new crystal defects. These formations of localized energy state and decrease band gap energy promote another pathway of transition [26].

Scanning electron microscopic studies was performed to find out the morphology and size of the prepared composites particle. Reduced graphene oxide, layers of $\text{WO}_3/\text{rGO}/\text{WO}_3$ and $\text{CoWO}_4/\text{rGO}/\text{CoWO}_4$ composites SEM images are presented in Fig. 3. The SEM image of reduced graphene oxide (Fig. 3a) clearly shows a reduced graphene oxide presented in wrinkled structure. Layered $\text{WO}_3/\text{rGO}/\text{WO}_3$ composite SEM (Fig. 3b) image confirms the tungsten oxide nanoparticles are coated over the reduced graphene oxide layer. Prepared $\text{WO}_3/\text{rGO}/\text{WO}_3$ composite shows a porous and irregular shape of

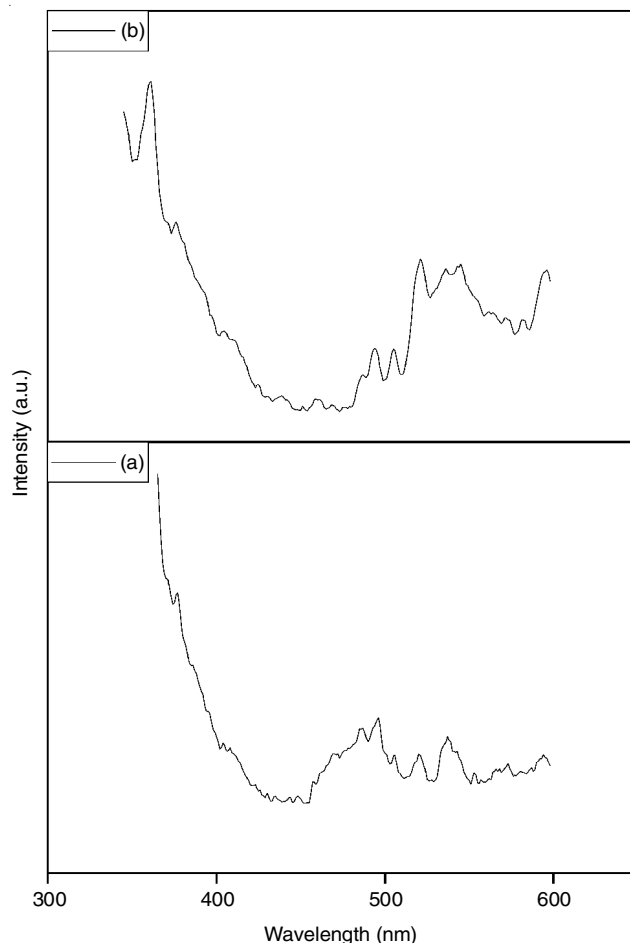


Fig. 2. Photoluminescence spectra of (a) $\text{WO}_3/\text{rGO}/\text{WO}_3$ and (b) $\text{CoWO}_4/\text{rGO}/\text{CoWO}_4$ composite

tungsten oxide nanoparticles and also tungsten oxide nanoparticles aggregate together to form the clusters over the surface rGO. Fig. 3c represents a SEM image of layered $\text{CoWO}_4/\text{rGO}/\text{CoWO}_4$ composite. The image clearly shows the prepared composite of $\text{CoWO}_4/\text{rGO}/\text{CoWO}_4$ are composed of nano sized CoWO_4 particles (60-80nm) and CoWO_4 nanoparticles are uniformly coated over the rGO layer.

Cyclic voltammetry (CV) technique was used to find out the electrochemical performance of the prepared electrode materials. Cyclic voltammetry was performed at -0.8 to 0.8 V, 2 M Na_2SO_4 used as an electrolyte of the prepared composite. Fig. 4(a) reveals the CV curves of prepared layer composites of $\text{WO}_3/\text{rGO}/\text{WO}_3$ and $\text{CoWO}_4/\text{rGO}/\text{CoWO}_4$ measured at scan rate of 100 mV s^{-1} in 2 M Na_2SO_4 aqueous electrolyte. Both composites show a nearly rectangular shape and small humps in the curves and indicate composites have a both electric double layer capacitance and pseudo capacitance properties. The high specific capacitance of layered $\text{CoWO}_4/\text{rGO}/\text{CoWO}_4$ is inferred from its high integrated area in CV loop compare to that of $\text{WO}_3/\text{rGO}/\text{WO}_3$. The high specific capacitance is attributed to larger surface area of doped materials [27]. Owing to the layered structure, these materials posses good electrical conductivity, more active site, remarkable charge storage and effective redox reactions on the surface of layer. These properties influence the ion transport or charge transfer and determine the electrochemical properties of the material [28].

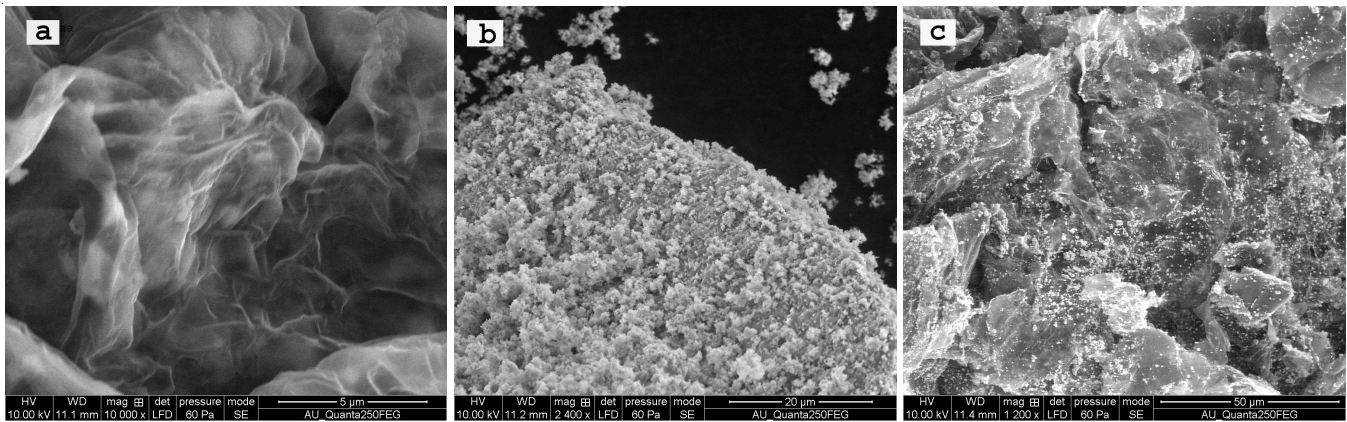


Fig. 3. SEM images of (a) rGO, (b) $\text{WO}_3/\text{rGO}/\text{WO}_3$, (c) $\text{CoWO}_4/\text{rGO}/\text{CoWO}_4$

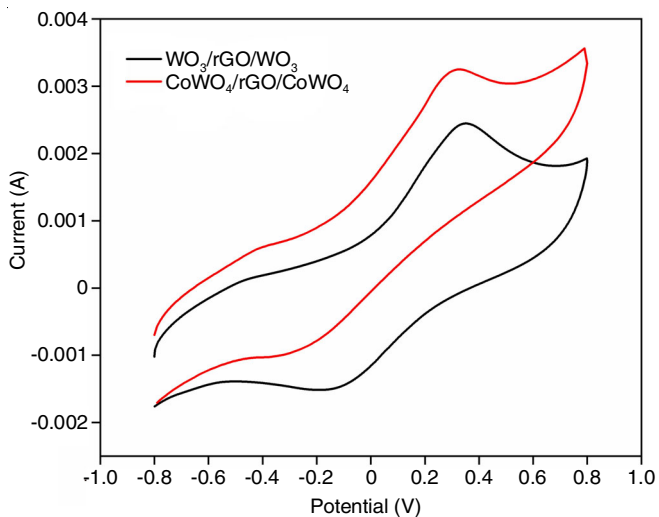


Fig. 4a. CV curves of $\text{WO}_3/\text{rGO}/\text{WO}_3$ and $\text{CoWO}_4/\text{rGO}/\text{CoWO}_4$ at 100 mV s^{-1}

Fig. 4(b-c) represents a CV curves of prepared $\text{WO}_3/\text{rGO}/\text{WO}_3$ and $\text{CoWO}_4/\text{rGO}/\text{CoWO}_4$ composites carried out at different scan rate of 5, 10, 20, 50 and 100 mV s^{-1} . For the scan rate 5, 10, 20, 50 and 100 mV s^{-1} , the specific capacitance of the $\text{WO}_3/\text{rGO}/\text{WO}_3$ composite and $\text{CoWO}_4/\text{rGO}/\text{CoWO}_4$ composite are exhibit a 283.5 , 187.6 , 78.9 , 52.6 and 39.6 Fg^{-1} and 500.9 , 155 , 94.5 , 48.7 and 36.4 Fg^{-1} , respectively. As prepared composites humps shifted towards to higher potential with increase of scan rate because charge polarization of the electrode. $\text{CoWO}_4/\text{rGO}/\text{CoWO}_4$ composite has higher specific capacitance 500.9 Fg^{-1} compare with $\text{WO}_3/\text{rGO}/\text{WO}_3$ composite 283.5 Fg^{-1} . The higher specific capacitance may be attributed to higher active sites and better charge storage capacity of layered $\text{CoWO}_4/\text{rGO}/\text{CoWO}_4$ [29].

Prepared electrode material conductivity behaviour was characterized using electrochemical impedance spectroscopy (EIS). Nyquist plots (Fig. 5) consist of three frequency region high frequency, intermediate and low frequency regions. At high frequency impedance curve intercept with the real axis represents a combination resistance of contact resistance at electrode, ionic resistance of electrolyte and intrinsic resistance of substrate. Impedance curve form semicircle in intermediate region and diameter of the semicircle represents a charge transfer resistance. The straight line appeared at low frequency region represents the Warburg impedance [30]. Electrical series resis-

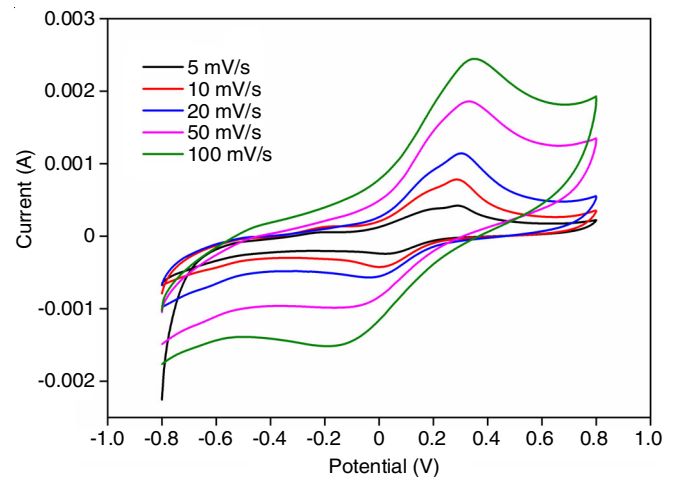


Fig. 4b. Cyclic voltammograms of $\text{WO}_3/\text{rGO}/\text{WO}_3$ at various scan rates

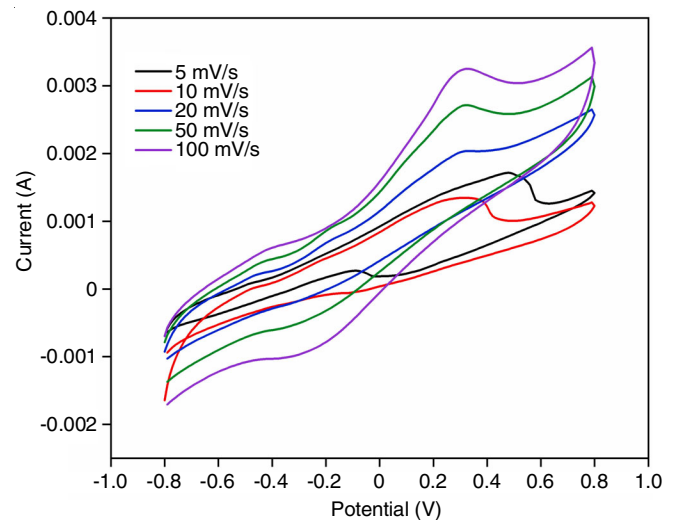


Fig. 4c. Cyclic voltammograms of $\text{CoWO}_4/\text{rGO}/\text{CoWO}_4$ at various scan rates

tance of undoped and doped composite is 8.7 and 7.9Ω , respectively. The semicircle diameter of the $\text{CoWO}_4/\text{rGO}/\text{CoWO}_4$ is smaller than that of $\text{WO}_3/\text{rGO}/\text{WO}_3$ composite indicates the smallest interfacial resistance and thus a good electrical conductivity for $\text{CoWO}_4/\text{rGO}/\text{CoWO}_4$ composite [31]. These results provide valuable information that $\text{CoWO}_4/\text{rGO}/\text{CoWO}_4$ composite has enhanced electrochemical properties compare with $\text{WO}_3/\text{rGO}/\text{WO}_3$ composite.

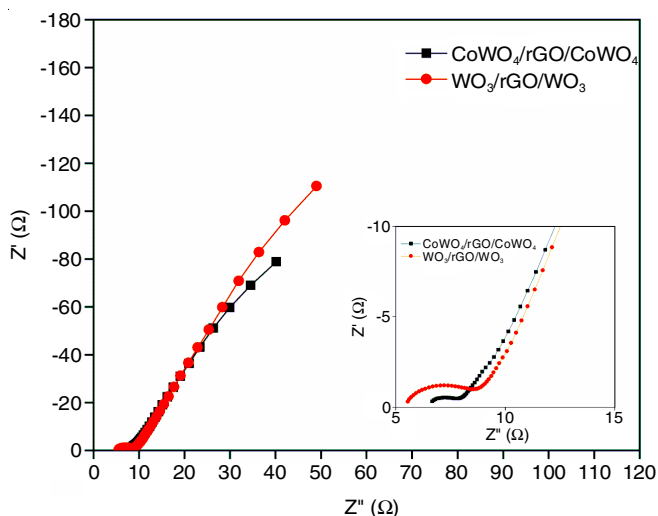


Fig. 5. Nyquist plot of $\text{WO}_3/\text{rGO}/\text{WO}_3$ and $\text{CoWO}_4/\text{rGO}/\text{CoWO}_4$ composites

Conclusion

Layered $\text{WO}_3/\text{rGO}/\text{WO}_3$ and $\text{CoWO}_4/\text{rGO}/\text{CoWO}_4$ composites were prepared using jet nebulized spray pyrolysis technique. The $\text{WO}_3/\text{rGO}/\text{WO}_3$ and $\text{CoWO}_4/\text{rGO}/\text{CoWO}_4$ composite materials show a crystalline nature with tetragonal phase and monoclinic phase, respectively. Band gap energy was calculated using photoluminescence spectra and found that band gap energy is lower (2.38 eV) for doped composite than the undoped composite (2.48 eV). SEM confirms metal oxide nanoparticles are coated over the reduced graphene oxide layer and nanoparticles are in the range of 60-90 nm. Electrochemical properties of the prepared composite were analyzed in CV and EIS. Cyclic voltammetric results reveal layered composites have synergistic effect of both EDLC and pseudo capacitance. ESR of the doped and undoped composites is 7.9 and 8.7 Ω , respectively. $\text{CoWO}_4/\text{rGO}/\text{CoWO}_4$ composite have a lower electrical series resistance compare with $\text{WO}_3/\text{rGO}/\text{WO}_3$ composite. This result indicates layered $\text{CoWO}_4/\text{rGO}/\text{CoWO}_4$ composite shows a better electrochemical performance compare with $\text{WO}_3/\text{rGO}/\text{WO}_3$ composites.

ACKNOWLEDGEMENTS

The authors acknowledge UGC (F.No.: 4-4/2013-14-MRP-SEM/UGC-SERO) for instrumental facility. The author also thanks Alagappa University, Karaikudi and Gandhigram University, Dindigul, India for material characterization analyses.

CONFLICT OF INTEREST

The authors declare that there is no conflict of interests regarding the publication of this article.

REFERENCES

- H.R. Naderi, A. Sobhani-Nasab, M. Rahimi-Nasrabadi and M.R. Ganjali, *Appl. Surf. Sci.*, **423**, 1025 (2017); <https://doi.org/10.1016/j.apsusc.2017.06.239>
- Z.S. Iro, C. Subramani and S.S. Dash, *Int. J. Electrochem. Sci.*, **11**, 10628 (2016); <https://doi.org/10.20964/2016.12.50>
- Z.K. Ghouri, M.S. Akhtar, A. Zahoor, N.A.M. Barakat, W. Han, M. Park, B. Pant, P.S. Saud, C.H. Lee and H.Y. Kim, *J. Alloys Compd.*, **642**, 210 (2015); <https://doi.org/10.1016/j.jallcom.2015.04.082>
- S.-M. Chen, R. Ramachandran, V. Mani and R. Saraswathi, *Int. J. Electrochem. Sci.*, **9**, 4071 (2014).
- G. Hu, C. Tang, C. Li, H. Li, Y. Wang and H. Gong, *J. Electrochem. Soc.*, **158**, A695 (2011); <https://doi.org/10.1149/1.3574021>
- S. Jiang, G. Yuan, C. Hua, S. Khan, Z. Wu, Y. Liu, J. Wang, C. Song and G. Han, *J. Electrochem. Soc.*, **164**, H896 (2017); <https://doi.org/10.1149/2.1231713jes>
- C. Yuan, H.B. Wu, Y. Xie and X.W.D. Lou, *Angew. Chem. Int. Ed.*, **53**, 1488 (2014); <https://doi.org/10.1002/anie.201303971>
- X.-H. Guan, X. Lan, X. Lv, L. Yang and G.-S. Wang, *Chemistry Select*, **3**, 6719 (2018); <https://doi.org/10.1002/slct.201800684>
- E.R. Ezeigwe, P.S. Khiew, C.W. Siong, I. Kong and M.T.T. Tan, *Ceram. Int.*, **43**, 13772 (2017); <https://doi.org/10.1016/j.ceramint.2017.07.092>
- Q. Ke and J. Wang, *J. Materiomics*, **2**, 37 (2016); <https://doi.org/10.1016/j.jmat.2016.01.001>
- F.O. Ochai-Ejeh, M.J. Madito, D.Y. Momodu, A.A. Khaleed, O. Olaniyan and N. Manyala, *Electrochim. Acta*, **252**, 41 (2017); <https://doi.org/10.1016/j.electacta.2017.08.163>
- P.Y. Chan and S.R. Majid, eds.: I. Ahmad and P. Di Sia, Metal Oxide-Based Electrode Materials for Supercapacitor Applications, In: Advanced Materials and their Applications-Micro to Nanoscale, One Central Press (OCP), Ch. 2, pp. 13-30 (2017).
- S. Ramkumar and G. Rajarajan, *Appl. Phys., A Mater. Sci. Process.*, **123**, 401 (2017); <https://doi.org/10.1007/s00339-017-0983-5>
- A. Lakehal, B. Bedhraf, A. Bouaza, B. Hadj, A. Ammari and C. Dalache, *Mater. Res.*, **21**, e20170545 (2018); <https://doi.org/10.1590/1980-5373-mr-2017-0545>
- R.L. Moreira, R.M. Almeida, K.P.F. Siqueira, C.G. Abreu and A. Dias, *J. Phys. D Appl. Phys.*, **49**, 045305 (2016); <https://doi.org/10.1088/0022-3727/49/4/045305>
- C. Zhang, D. Guo, C. Hu, Y. Chen, H. Liu, H. Zhang and X. Wang, *Phys. Rev. B*, **87**, 035416 (2013); <https://doi.org/10.1103/PhysRevB.87.035416>
- E. Mitchell, J. Candler, F. De Souza, R.K. Gupta, B.K. Gupta and L.F. Dong, *Synth. Met.*, **199**, 214 (2015); <https://doi.org/10.1016/j.synthmet.2014.11.028>
- F. Li, H.Y. Na, W. Jin, X. Xu, W. Wang and J. Gao, *J. Solid State Electrochem.*, **22**, 2767 (2018); <https://doi.org/10.1007/s10008-018-3962-7>
- T. Lee, T. Yun, B. Park, B. Sharma, H.-K. Song and B.-S. Kim, *J. Mater. Chem.*, **22**, 21092 (2012); <https://doi.org/10.1039/c2jm33111j>
- N. Sethupathi, P. Thirunavukkarasu, V.S. Vidhya, R. Thangamuthu, G.V.M. Kiruthika, K. Perumal, H.C. Bajaj and M. Jayachandran, *J. Mater. Sci. Mater. Electron.*, **23**, 1087 (2012); <https://doi.org/10.1007/s10854-011-0553-0>
- M. Jana, S. Saha, P. Samanta, N.C. Murmu, N.H. Kim, T. Kuila and J.H. Lee, *J. Power Sources*, **340**, 380 (2017); <https://doi.org/10.1016/j.jpowsour.2016.11.096>
- V.H. Pham, T.-D. Nguyen-Phan, X. Tong, B. Rajagopalan, J.S. Chung and J.H. Dickerson, *Carbon*, **126**, 135 (2018); <https://doi.org/10.1016/j.carbon.2017.10.026>
- H. Saleem, M. Haneef and H. Abbasi, *Mater. Chem. Phys.*, **204**, 1 (2018); <https://doi.org/10.1016/j.matchemphys.2017.10.020>
- V. Hariharan, V. Aroulmoji, K. Prabakaran, M. Parthibavarman, B. Gnanavel, R. Sathyapriya and M. Kanagaraj, *J. Alloys Compd.*, **689**, 41 (2016); <https://doi.org/10.1016/j.jallcom.2016.07.136>
- L. Zhang, S. Song and H. Shi, *J. Alloys Compd.*, **751**, 69 (2018); <https://doi.org/10.1016/j.jallcom.2018.04.109>
- K. Sathishkumar, N. Shanmugam, N. Kannadasan, S. Cholan and G. Viruthagiri, *J. Mater. Sci. Mater. Electron.*, **26**, 1881 (2015); <https://doi.org/10.1007/s10854-014-2624-5>
- I.A. Dhole, Y.H. Navale, Y.M. Jadhav, R.N. Mulik, S.G. Pawar, C.S. Pawar and V.B. Patil, *AIP Conf. Proc.*, **1989**, 020011 (2018); <https://doi.org/10.1063/1.5047687>
- Y. Guo, Y. Wei, H. Li and T. Zhai, *Small*, **13**, 1701649 (2017); <https://doi.org/10.1002/smll.201701649>
- S. Kulandaivalu, N. Suhaimi and Y. Sulaiman, *Sci. Rep.*, **9**, 4884 (2019); <https://doi.org/10.1038/s41598-019-41203-3>
- Rusi and S.R. Majid, *PLoS ONE*, **11**, e0154566 (2015) <https://doi.org/10.1371/journal.pone.0154566>
- P. Liu, J. Yan, X. Gao, Y. Huang and Y. Zhang, *Electrochim. Acta*, **272**, 77 (2018); <https://doi.org/10.1016/j.electacta.2018.03.198>